

A MICROWAVE RESONATOR
INVESTIGATION OF ELECTRIC FIELD
EFFECTS ON MERCURY SURFACES

by

GEORGE NICOS IONIDES

B.Sc., University of London, 1968

A THESIS SUBMITTED IN PARTIAL FULFILMENT OF
THE REQUIREMENTS FOR THE DEGREE OF
MASTER OF SCIENCE
in the Department
of
PHYSICS

We accept this thesis as conforming to the
required standard

THE UNIVERSITY OF BRITISH COLUMBIA

December, 1969

In presenting this thesis in partial fulfilment of the requirements for an advanced degree at the University of British Columbia, I agree that the Library shall make it freely available for reference and study.

I further agree that permission for extensive copying of this thesis for scholarly purposes may be granted by the Head of my Department or by his representatives. It is understood that copying or publication of this thesis for financial gain shall not be allowed without my written permission.

Department of PHYSICS

The University of British Columbia
Vancouver 8, Canada

Date 13th Jan. 1970

ABSTRACT

The microwave resonator method for studying small amplitude surface waves in liquids has been improved by making the time measurement more accurate and much more convenient. It was used to measure the oscillation frequency of the surface as a function of liquid depth. Discrepancies between the experimentally obtained results and theoretical predictions due to the rigidity of the mercury meniscus where contact is made with the walls of a cylindrical resonator were found. From these an accurate value for the effective reduction in radius of the resonator because of the meniscus effect was obtained. A method was developed for applying strong electrostatic fields (about 20 kV/cm) onto the fluid surface without interfering with the measuring technique. An interesting result of this was the observation that the field cleans the surface from contamination. This phenomenon manifests itself in a marked reduction in the damping of surface waves just after a large field is applied. A resonator of square cross-section was used to demonstrate the Fourier analyzing property of rectangular resonators.

TABLE OF CONTENTS

	Page
ABSTRACT	(ii)
TABLE OF CONTENTS	(iii)
LIST OF TABLES	(iv)
LIST OF FIGURES	(v)
ACKNOWLEDGEMENTS	(vi)
CHAPTER 1 INTRODUCTION	1
CHAPTER 2 EQUIPMENT - EXPERIMENTAL PROCEDURE	
2.1 Microwave arrangement and test cavity	5
2.2 Refinement of timing technique	12
2.3 Application of an electrostatic field on the mercury surface	17
CHAPTER 3 RESULTS	
3.1 Variation of surface mode frequency with fluid depth	20
3.2 Effects of a strong electrostatic field on the mercury surface	24
3.3 The rectangular cavity	30
CHAPTER 4 CONCLUSIONS-- FUTURE WORK	
4.1 Improvement of measuring technique	36
4.2 Application of a strong electric field on the fluid surface	36
4.3 Effect of the electric field on the mercury surface	37
4.4 The square resonator	37
4.5 Seismographic applications of the microwave resonator	38
REFERENCES	39
APPENDIX THEORY OF THE CLEANING OF THE MERCURY SURFACE BY AN ELECTRIC FIELD	40

LIST OF TABLES

		Page
1	Oscillation frequency measurements.	22
2	Parameters and variables employed.	22
3	Surface wave damping coefficient results.	28

LIST OF FIGURES

	Page
1 The microwave system	6
2 EM mode frequency measurement	7
3 Cavity resonator and accessories	9
4 The lid of the cylindrical cavity	10
5a,b Arrangement for exciting surface waves by periodic air pulses	11
6 Monitoring of the amplitude and frequency of a surface mode	13
7 Arrangement for generating time marks	15
8 Trigger pulse amplifier	15
9 Time marks recorded directly on the film	16
10 Application of a strong electrostatic field on the mercury surface	19
11 Surface mode frequency vs. fluid depth plot	23
12 Damping of a surface wave	26
13 Contamination of the mercury surface	28
14 The rectangular resonator	31
15 Simultaneous display of EM modes on the screen	32
16 The lid of the rectangular resonator	34
17 Selective response of EM to surface modes	35
18 Response of both EM modes to a surface mode	35
19 A collapsed monolayer of oil on the mercury surface	42
20a,b Removal of thin oil film by a strong electric field	42
21 Weight and string analogue of the breaking up of the oil film	42

ACKNOWLEDGEMENTS

I would sincerely like to thank Dr. F. L. Curzon for the stimulating and encouraging supervision that I received throughout the course of this work. I wish to express my appreciation to Dr. B. Ahlborn for his suggestions on the improvement of the presentation of this thesis. I must also acknowledge numerous valuable discussions which I had with Mr. J.-P. Huni on both the theoretical and the experimental aspects of this work.

I am indebted to Mr. R. Haines for his guidance during my familiarization with the student workshop. Special thanks are due to Mr. D. Sieberg, Mr. J. A. Zanganeh and Mr. R. Da Costa for their assistance with the electronics and in the general maintenance of the equipment.

Finally, I must express my gratitude to the Graduate School of the University of British Columbia for financial assistance through the award of a University of British Columbia Graduate Fellowship.

CHAPTER 1

I N T R O D U C T I O N

Experimental investigations of surface waves in liquids have, until recently, been hampered by the lack of a suitable diagnostic technique. Most electromechanical sensing devices developed over the years had the disadvantage of being too insensitive to permit observations of linear surface waves (i.e. periodic oscillations for which the product $\xi \lambda^2 H^{-3}$ is very small compared to unity, where ξ is the amplitude, λ the wavelength of the surface waves, and H the depth of the liquid). But, as is well known, a satisfactory general theory (i.e. non-linear) for surface waves in fluids does not exist at present because of the enormous complexity of the resulting general equations. So, with the exception of a few very special cases, in which other simplifying conditions exist that render the equations "manipulatable", it is not, in general, possible to compare experimental results with existing theory. Optical techniques, due to their generally high spatial resolution, do not present us with the problem of insensitivity (in fact holographic methods are even too sensitive) but again cannot be considered fully satisfactory for the following reasons. They are difficult and complicated to set up and comparatively costly; also, together with the first class of sensing devices mentioned, they can in general only be employed to observe periodic phenomena (i.e. no continuous

observation of surface instabilities is possible). However, as was suggested by Curzon and Howard, and developed by Curzon and Pike (refs. 2,3,4,5), a microwave resonator technique can be employed which does not suffer from the drawbacks of previous methods. The most important features of this method are

- 1) Waves of small amplitude (10^{-3} cm) can be studied (i.e. linearized equations are applicable).
- 2) Unstable surfaces can be observed (i.e. non-periodic perturbations).
- 3) Under special circumstances the resonator responds to single modes of surface waves. This eliminates the tedious Fourier analysis which is normally required in comparing observations with theoretical predictions.

The principle of the technique is the following. If the boundaries of a resonating microwave cavity are perturbed a change in the resonant frequency results. Thus if one wall of a microwave cavity resonator is taken by a conducting liquid, any small surface perturbations of the fluid can easily be monitored by monitoring the resonant frequency changes of the cavity. Calculations of the shift in resonance are done by using Slater's theorem (ref. 6). It can be shown (see ref. 2, p. 10-13) that for a cylindrical and a rectangular microwave resonator the shift in frequency for a given surface mode of oscillation and a given electromagnetic mode is proportional to the amplitude of the surface wave. The method was developed by Pike using mercury

as the conducting liquid. He checked the theoretically predicted values of the oscillation frequency of a surface standing wave, both as a function of radius of a cylindrical microwave resonator and as a function of depth of the fluid. He also studied the damping of the surface waves, with and without an axial magnetic field acting on the mercury.

The work reported in this thesis is a follow up of the original investigations. The time measuring technique has been improved and the feasibility of applying a strong electric field on the mercury surface has been demonstrated, our ultimate future goal being the study of electrostatic-hydrodynamic instabilities. These are the instabilities that arise when a strong electric field is applied on the surface of an oscillating conducting liquid (see ref. 7). As a by-product of this investigation, a technique was found for removing impurities (e.g. small dust particles or traces of oil) from the surface of the mercury by applying a strong electrostatic field for a short period of time on the surface. This is extremely useful because even minute amounts of impurities on the surface of a liquid have a very drastic effect on the properties of the surface. Lastly, the feasibility of employing a rectangular cavity to Fourier analyse the surface wave modes was demonstrated.

In the calculations in the thesis the rationalised MKS system of units was used. To save unnecessary and ir-

repetitive repetition of the same long words the following nomenclature will be consistently used through out. "Surface modes" will be used to refer to any modes of oscillation of the mercury surface and "EM modes" for the resonant electromagnetic modes of the microwave resonator.

CHAPTER 2

EQUIPMENT EXPERIMENTAL PROCEDURE

2.1 A block diagram of the microwave system is shown in fig. 1. A 723 A/B Klystron produces 8.6 to 9.6 KMc/s microwaves. These go through an isolator whose purpose is to prevent any stray reflections from the rest of the system from interfering with the klystron output. They then go through a calibrated wavemeter which can be used to give the frequency of the microwave resonances. Lastly, the microwave signal is split into two parts of equal power at a magic tee. One of these component signals goes to the cavity, while the other half is dissipated in the terminator. The reflected signal from the cavity is picked up by a crystal detector and displayed on one channel of a dual beam oscilloscope. The time-base waveform of the oscilloscope is added to the klystron repeller voltage, thereby modulating the output frequency of the klystron. In this way, the time axis of the oscillograms can be calibrated directly in terms of the output frequency of the klystron. At the resonant frequencies of the microwave cavity a drop in the oscillogram is seen on the oscilloscope screen. The resonant frequency can be accurately measured by bringing the corresponding drop (or dip) in the signal due to the wavemeter into coincidence with the cavity dip (see fig. 2). The microwave

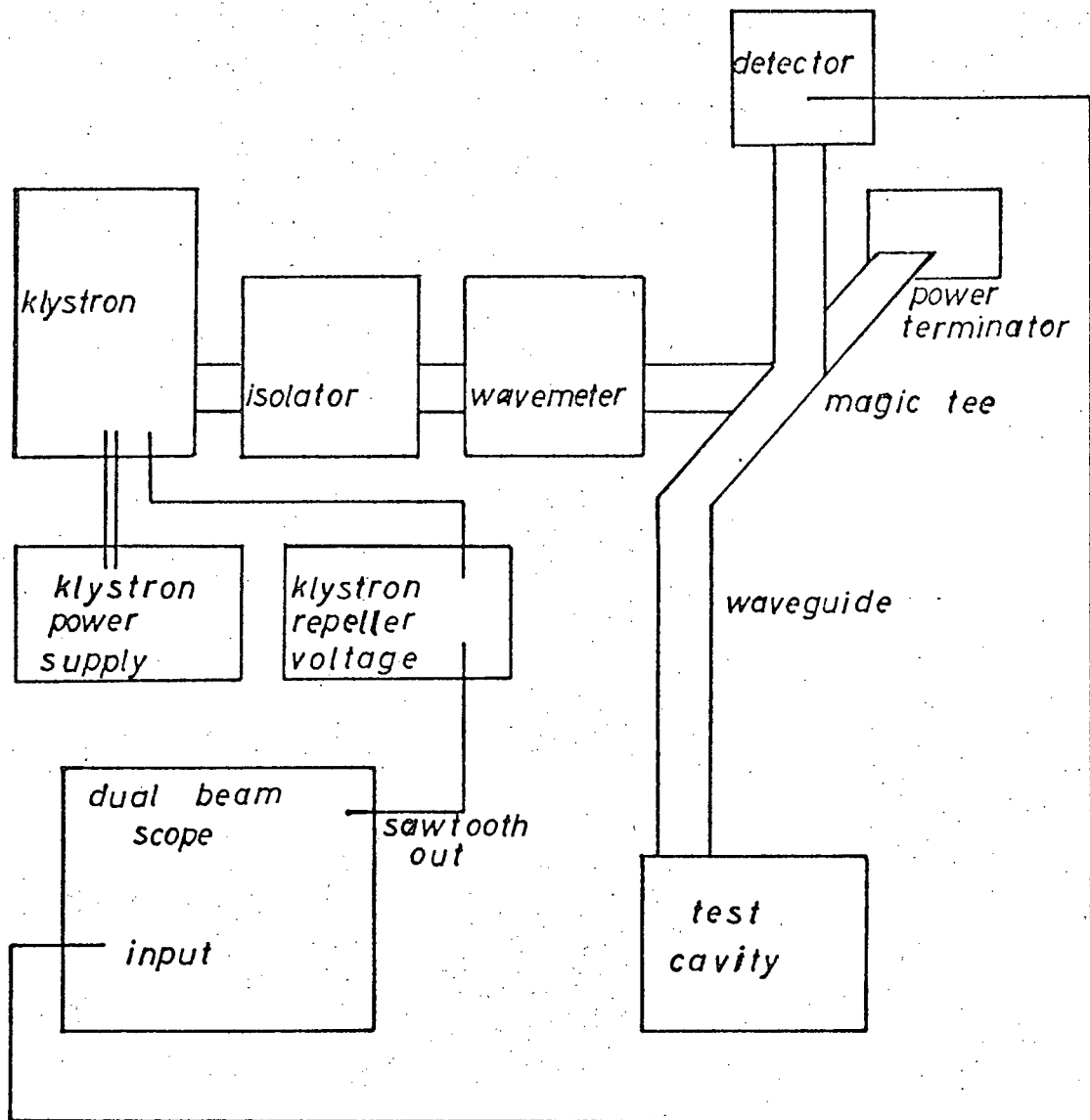


FIG 1
Block diagram of microwave set up.

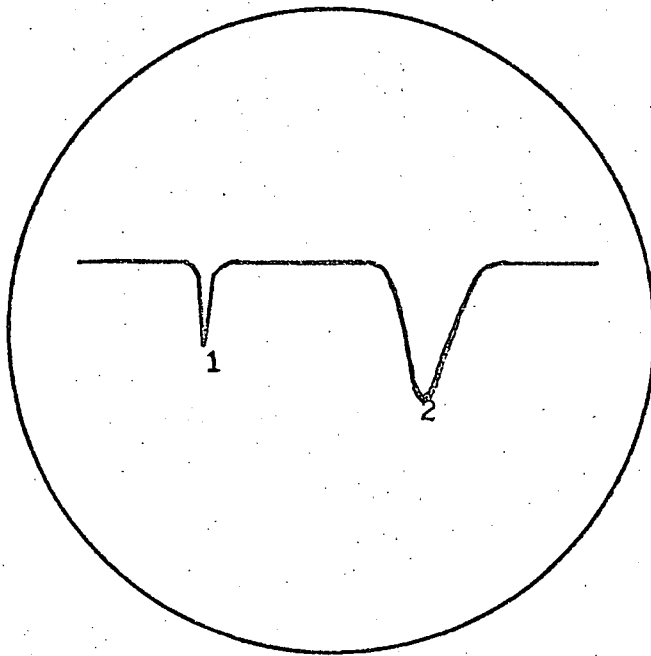


FIG 2

Measurement of the resonant frequency of an EM mode in the cavity.

Dip 1 is due to the calibrated wave-meter and can be moved right across the frequency spectrum of the klystron. Dip 2 is a typical example of a cavity EM mode resonance. For our experiments we used a klystron frequency range of from 8715 Mc/s to 8745 Mc/s.

cavity consists of a nickel plated brass cylinder shown in fig. 3. The layer of nickel (0.003 in. thick) eliminates dissolution of the brass by the mercury. Mercury can be introduced at the bottom of the cavity; its level can be very finely adjusted by using a hose clip as a tap control on a small length of Tygon tubing connecting the mercury reservoir to the cavity. Since the resonant frequency of the EM modes is a function both of the radius R and the length L of the cavity, resonances are seen on the oscilloscope screen as the mercury level is gradually raised in the cavity. At a fixed cavity length the mercury depth can be varied by means of a plunger. The plunger is attached to a threaded rod, so it can be moved up and down. The threaded rod passes through a Teflon nut which provides an effective seal for the mercury (fig. 3). A brass plate, details of which are shown in figs. 3 and 4 is used as the top of the microwave cavity. The best method of exciting surface modes on the mercury was by pulsing air through a small hole at the top of the cavity. The periodic air pulses were produced by interrupting an air jet with a rotating slotted disc. The disc is electrically driven by a 1/20 hp Bodine electric motor. The speed can be controlled by varying the input voltage with a variac. A transistor potentiometer can be used for fine adjustment of the motor speed. This is necessary since the mercury surface has a fairly high Q factor (about 50). The whole arrangement is shown in fig. 5.

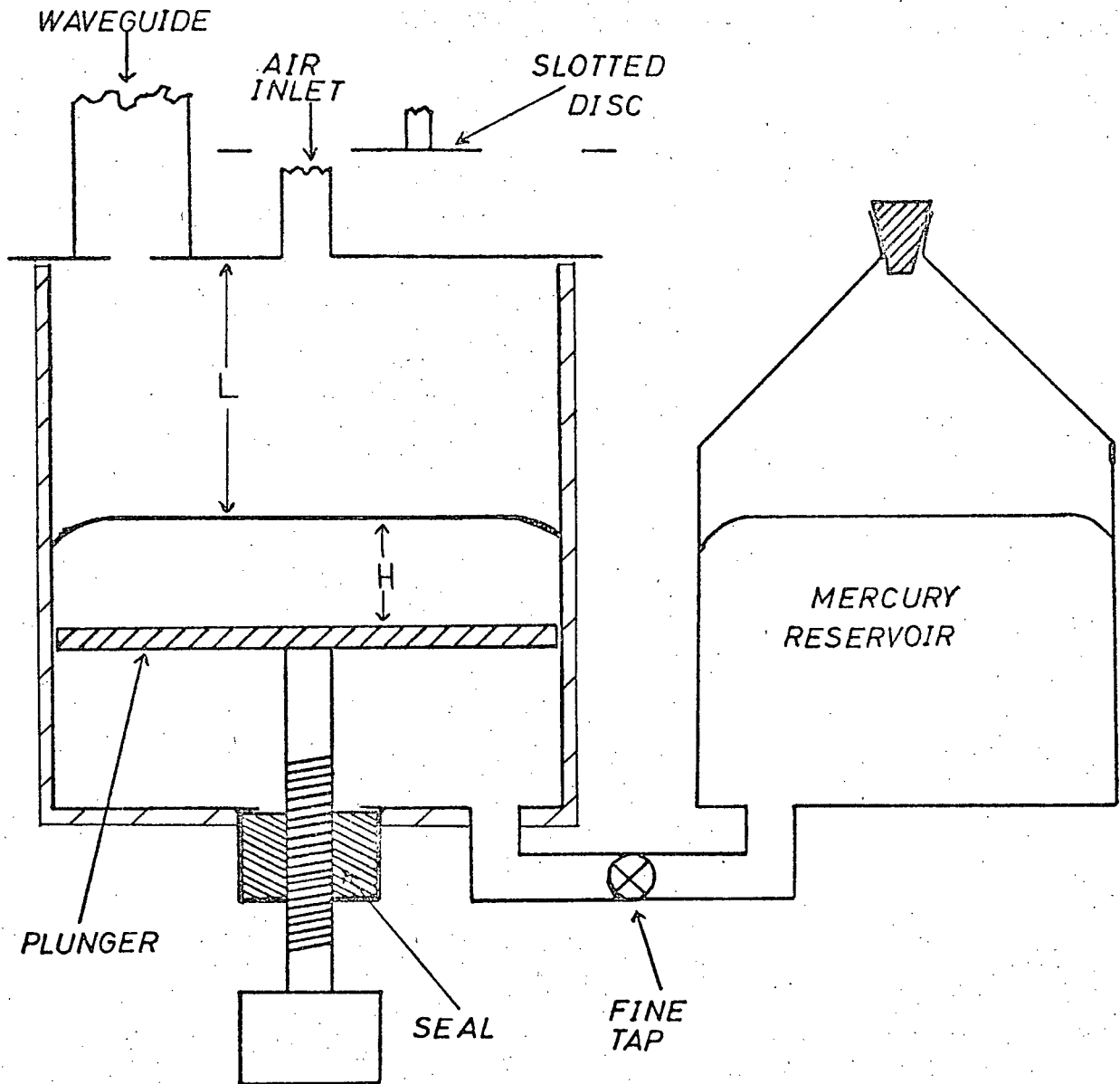


FIG 3

The microwave test cavity and mercury reservoir.

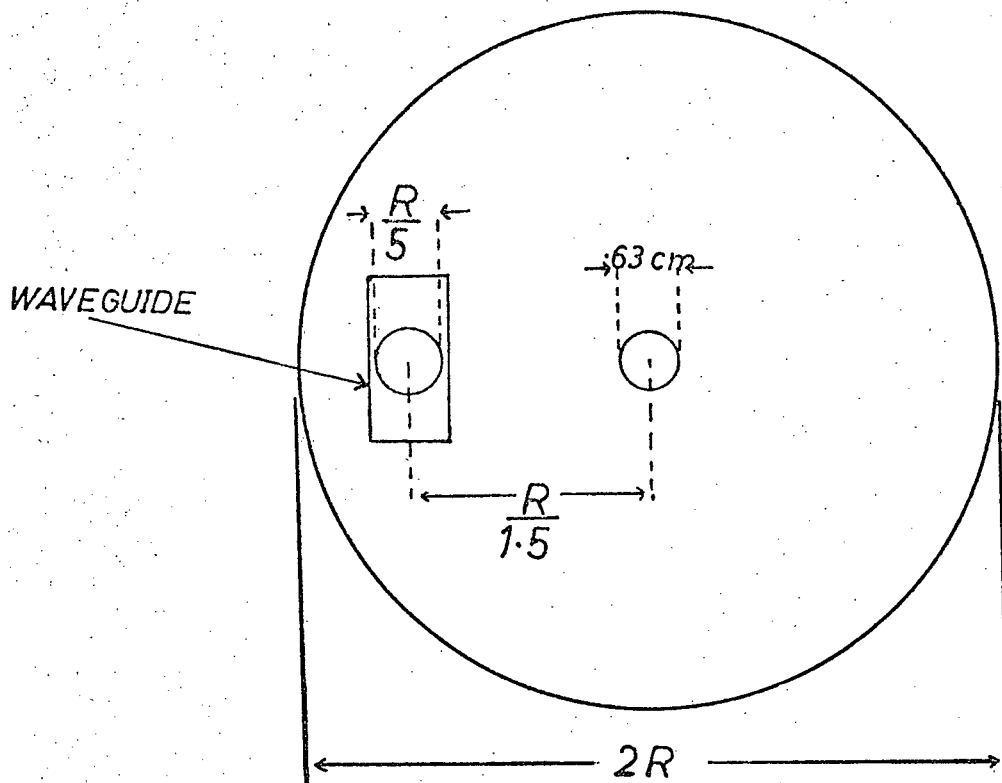


FIG 4

Details of the geometry of the lid of the cavity.

This arrangement gives best results of microwave resonances.

The waveguide is carefully soldered onto the top plate.

In our case, $R = 3.64 \text{ cm}$

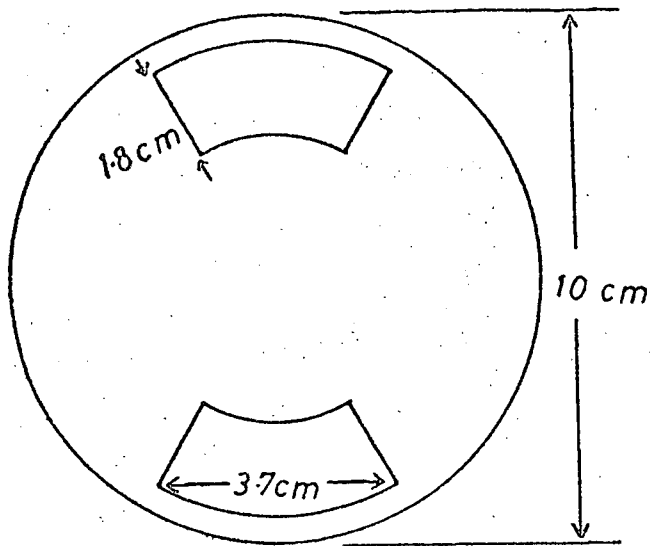


FIG 5a

Geometry of the
slotted disc.

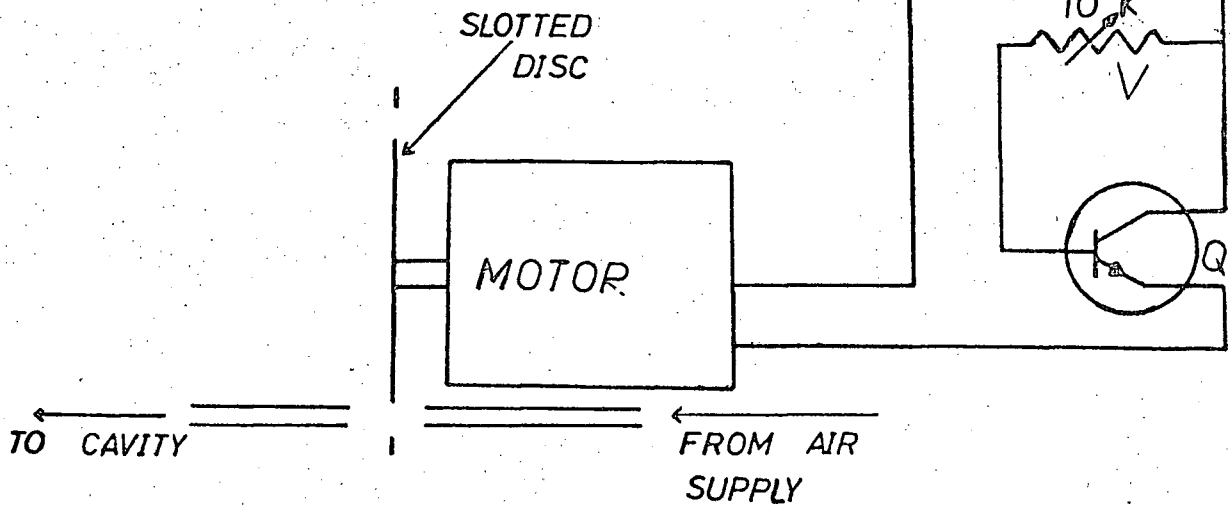


FIG 5b Motor control circuit. Air pulse arrangement.

V=VARIAC, BR=BRIDGE RECTIFIER

Q=2N3739 HEAT SUNK TRANSISTOR

Observations of the oscillation frequency and amplitude of the surface modes are made as follows. By virtue of the fact that our method of exciting surface modes excites only single modes, a time record of the periodic swinging of the EM mode resonance dip from the left to the right of the screen and back gives all the information needed. As was mentioned in Chapter 1, the amplitude of the wave is proportional to the resonant frequency shift. The oscillation frequency can be obtained by a simple time measuring technique which we shall elaborate on shortly. The time record is most conveniently made by putting a very narrow slit (about 0.5 mm) in front of the screen, as shown in fig. 6. Ordinary photographic film run in a direction perpendicular to the slit records the oscillations. A typical negative film record is shown in the same figure.

2.2. The measuring method and its refinement

The previously employed method for measuring time on the film was simply by triggering the oscilloscope with a time-mark generator. This results in the film record consisting of a series of dots (see fig. 6) whose spacing is equal to the repetition rate of the time-mark generator. Thus the period of the surface modes was found by counting the number of dots from peak to peak of the sinusoidal film trace. This method was extremely tedious and time consuming since the dots were counted by using a microscope. This had the serious disadvantage of causing considerable eye strain, not

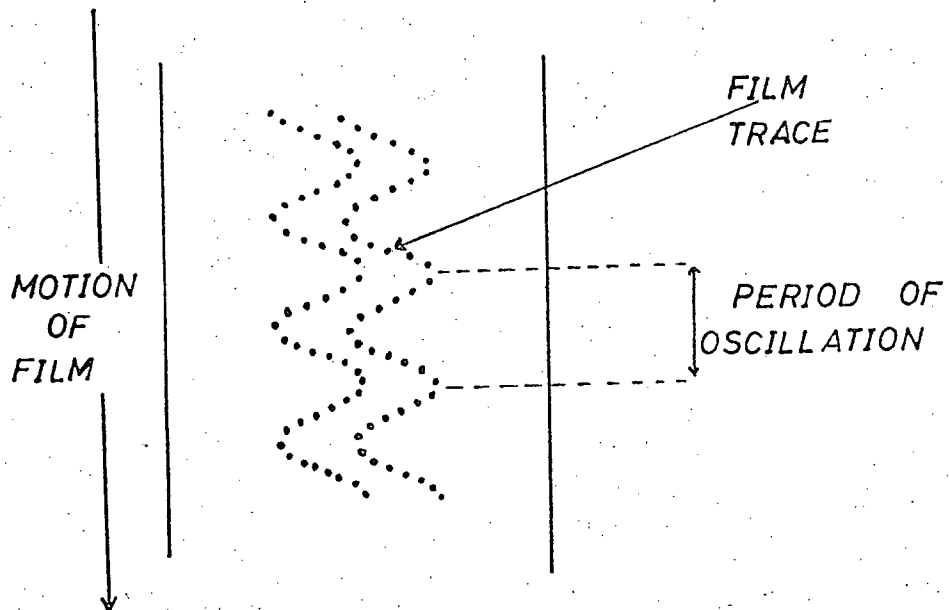
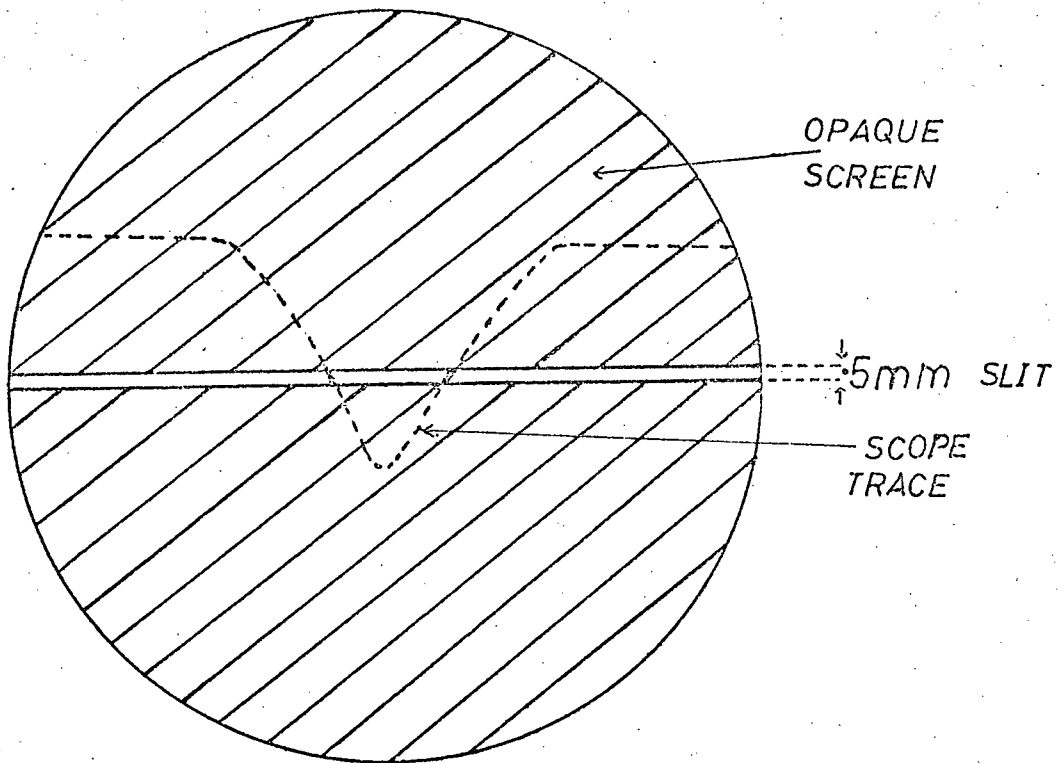


FIG 6

Method of monitoring the amplitude and frequency of a surface mode by recording the corresponding EM mode resonance shift.

to mention temporary mental derangement of the experimenter. To eliminate these difficulties we now record time marks directly on the film.

A Dumont type 781A time-mark generator (abbreviated in any future reference as a TMG) is used to give 1, 10 and 100 msec marks. These, in turn, are fed into three trigger pulse amplifiers (abbreviated to TPA) which amplify the signal to between 20 and 25 Volts. This level of signal is now sufficient to trigger three Tektronix type 163 pulse generators (abbreviated to PG) powered by a type 160A power supply. The resulting pulses are fed into the second channel of the dual beam oscilloscope. The oscilloscope is itself triggered externally by the 1 msec TMG marker. The whole arrangement, with the exception of power supplies is shown in block diagram form in fig. 7. Fig. 8 shows the TPA, designed and built by Mr. Jim A. Zanganeh to whom I am indebted.

All three pulses have the same amplitude, but the duration of the 100 msec pulse is twice as long as the duration of the 1 and 10 msec markers. As fig. 9 shows, the 1 msec marks appear at the left of the film. At 10 msec intervals, the 1 and 10 msec markers add, so that the top of the resultant marker is not observed in the slit across the face of the oscilloscope; i.e. every tenth marker is missing. At 100 msec all three markers coincide and add up except for the right hand half of the 100 msec marker pulse which is still visible in the slit. The resulting film is also shown in fig. 9.

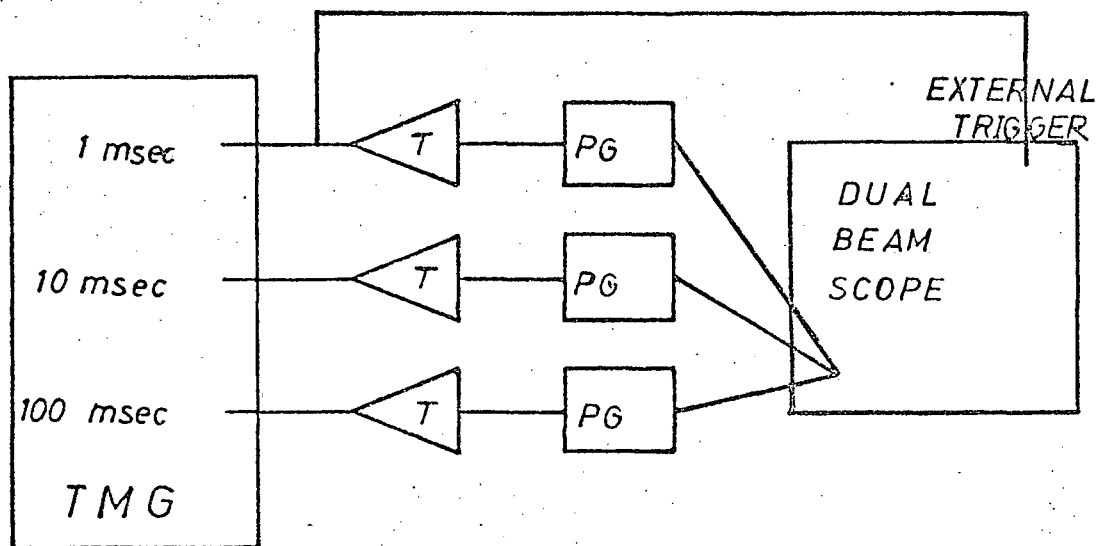


FIG 7 Arrangement for recording time marks

TMG=TIME MARK GENERATOR

T=TRIGGER PULSE AMPLIFIER

PG = PULSE GENERATOR

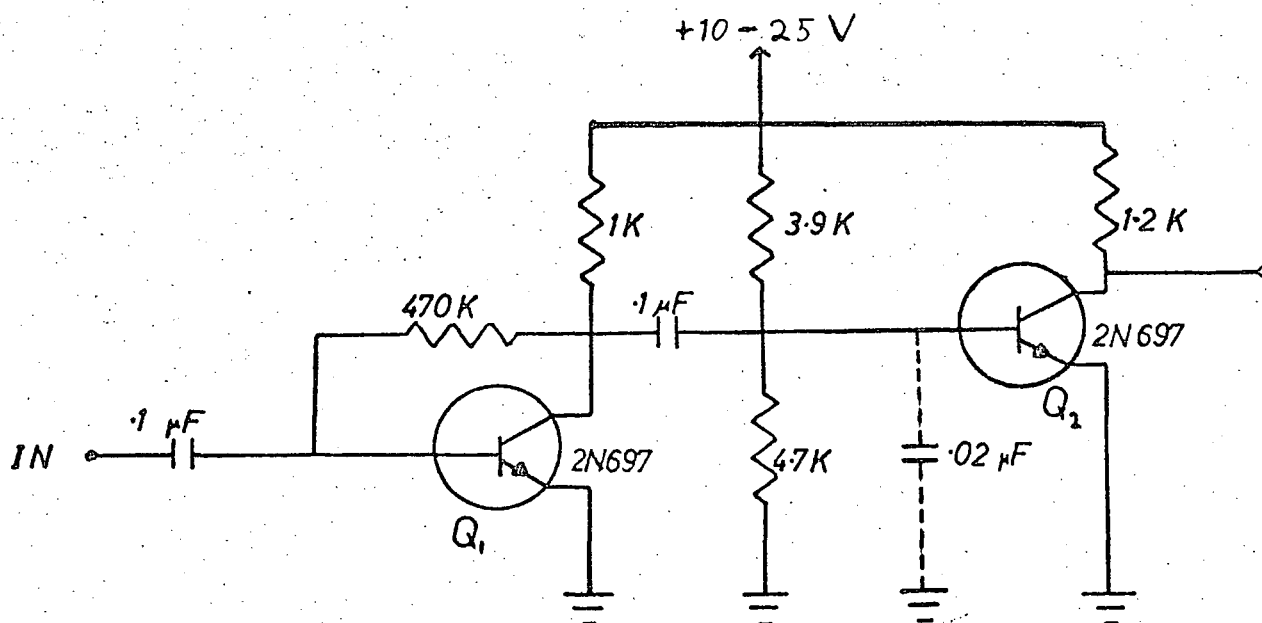


FIG 8

Trigger pulse amplifier circuit.

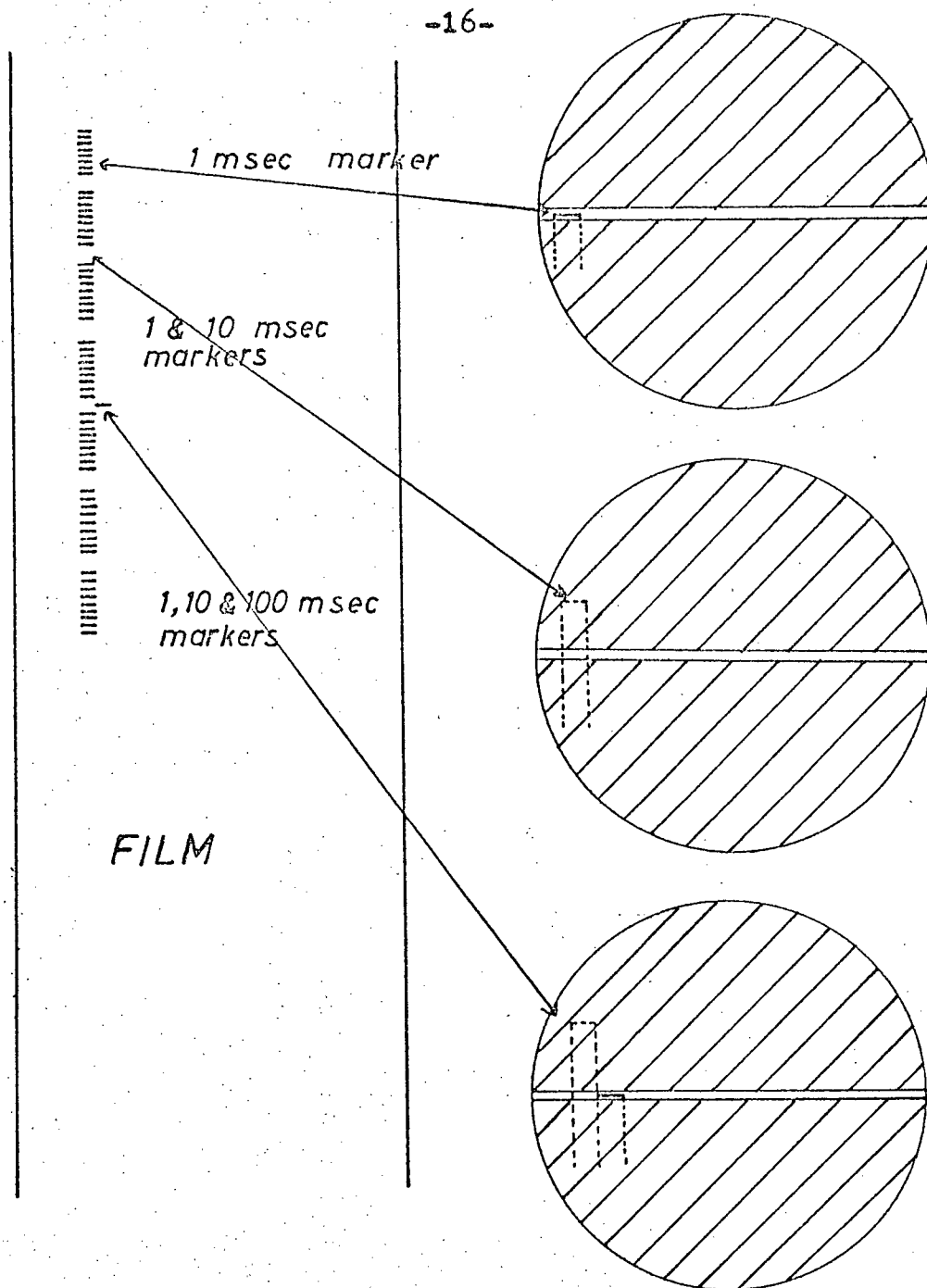


FIG 9

Method of recording time marks directly onto the film.

As it is easily seen, this method of measuring time is very convenient and much faster than the one employed before. It is also highly adaptable to measuring of any order, as long as time-marks are obtainable from the TMG. With the TMG and the oscilloscope employed, time intervals ranging from 1 microsecond up to 1 second can be accurately measured. An accuracy of 0.1% can be attained in the measurement of typical periodic times of surface modes. This is about ten times as accurate as the method used in the past.

2.3. Application of a strong electric field onto the mercury surface

One of the objectives of this work was to develop a method for applying a strong electrostatic field on the oscillating fluid. We also sought to find what effect, if any, the field would have on the properties of the surface itself. This means that an electric field must be applied between the top of the cavity and the base. To avoid perturbing the EM modes, any gap between the top of the cavity and the base must be kept to an absolute minimum. We therefore chose to insulate the base from the top of the cavity by using a suitable dielectric, hoping that microwave power losses in the dielectric would not reduce the Q-factor of the cavity EM modes too much. Mylar sheets proved to be the best for this purpose. Mylar has a dielectric strength of 4kV/0.001 inches. In our arrangement, four Mylar sheets

each 0.005 inches thick, providing an effective insulation of 80kV were used. No serious reduction in the cavity Q-factor was observed. A simple lucite clamp was used to keep the top plate in position over the cavity. Nylon screws, to avoid the possibility of breakdown, were employed to join the arms of the clamp together. A novel feature of the arrangement was the fact that surface modes could still be excited on the mercury, by pulsing the air above the Mylar. This demonstrates the fact that very little energy is required to excite surface modes and the very high sensitivity of the measuring technique. The largest of three available cavities, $R = 3.64\text{cm}$, was used for the electric field runs. The reason for this was the following. The distance between the mercury and the cavity lid was smaller for a given EM mode, than the corresponding distance in the other cavities. Hence the applied static electric field was also largest in this particular cavity for a given supply voltage. To avoid operating the microwave equipment at high potentials we grounded the lid of the cavity and connected the base to a 30kV power supply of negative output. Most of our measurements were done with this arrangement. However, in our final runs, a further increase of the electrostatic field strength was effected as follows. The method of putting Mylar in the path of the microwaves proved so effective and absorbed so little power that we extended it successfully to the microwave waveguides themselves. The microwave joint between the

wavemeter and the magic tee (see fig.1) was disconnected and two Mylar sheets were introduced. Again a lucite clamp with nylon screws was used to hold the joint together after insertion of the Mylar. Then, a second power supply, of positive output this time, was used to raise the cavity lid to positive 20kV. This arrangement of two power supplies in series enabled us to apply an effective potential difference of 50kV between the top and the base of the cavity. The set up is shown in fig. 10.

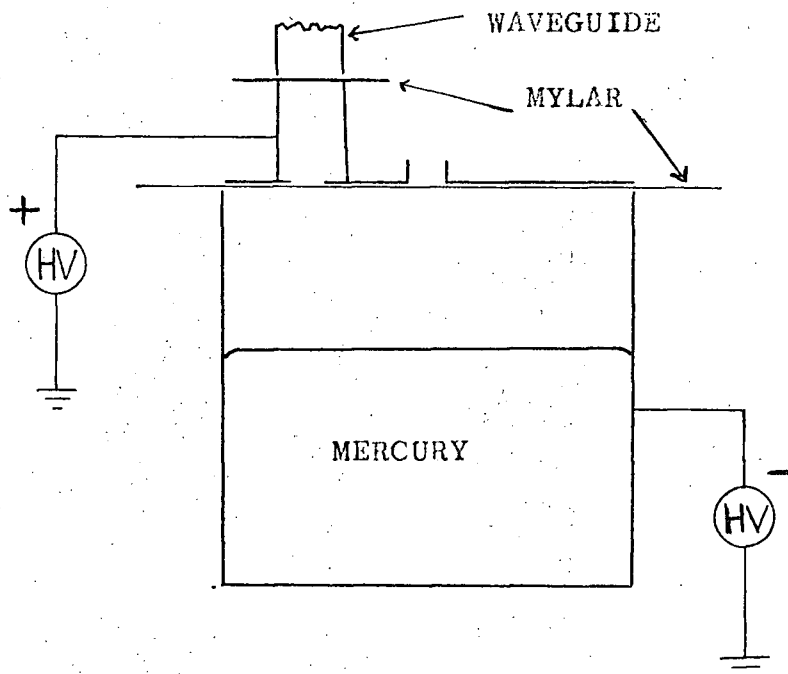


FIG 10

Method of application of a strong electric field on the mercury surface.

CHAPTER 3

R E S U L T S

3.1. Variation of the frequency of surface modes with depth

At first we compared theoretically predicted values of the frequency of surface modes as a function of depth with experimentally obtained values. This could be done much more reliably than before with our refined measuring technique.

The linearised theory of standing surface waves on a fluid surface gives the dispersion relation

$$(2\pi f)^2 = \left(\frac{T k^3}{\rho} + g k \right) \tanh(kH) \quad (3.1.1)$$

where T = surface tension of the liquid,

k = wave number of oscillations,

f = frequency of oscillations,

ρ = density of the liquid,

H = depth of the liquid,

and g = acceleration of gravity.

The vertical displacement ξ_z of the oscillating surface from the equilibrium position is given by (see ref. 8)

$$\xi_z = \sum \xi_{sv} J_s(kr) \cos(s\varphi) \quad (3.1.2)$$

where ξ_{sv} = amplitude of the oscillation,

$J_s(kr)$ = Bessel function of order s .

The boundary condition that $\frac{d\xi_z}{dr} \Big|_{r=R} = 0$ gives

$$K = j'_{sv} / R \quad (3.1.3)$$

where j'_{su} is the Uth positive root* of $J'_s(KR)=0$. The self-explanatory notation ξ_{su} will be used to refer to individual surface modes from now onwards.

Formula (3.1.1) was used to plot f vs. H . The experimentally obtained points are plotted from table 1 on the same graph (fig. 11). Table 2 gives the values of the parameters used in the experiment.

The ξ_{11} oscillation, with $k=0.507 \text{ cm}^{-1}$, was used. Curzon and Pike used the ξ_{02} mode and found discrepancies between experimental values of the frequency and values predicted by (3.1.1). To explain this, they reasoned that the mercury meniscus is very rigid at the edges, where the mercury comes into contact with the walls of the container. This brings about an effective reduction in R , as far as the surface modes are concerned. As can be seen from the graph, if R is reduced by 0.22 cm, corresponding to a new k of 0.54 cm^{-1} (from equation 3.1.3), there is excellent agreement between corrected theory and experiment.

Transverse electric EM modes were used in the experiment. Modes are defined in an exactly analogous manner in electrodynamics as surface modes were defined in (3.1.2).

* At this stage, we would like to point out to the reader, that although in their theory Curzon and Pike state that they use the Uth positive non-zero root, in the analysis of their results they use the same nomenclature as given here.

TABLE 1

Fluid Depth H cm	Oscillation frequency f c/s
0.49	1.83
0.62	2.04
0.74	2.22
0.8	2.31
0.99	2.53
1.08	2.61
1.19	2.76
1.53	2.97
1.96	3.20

TABLE 2

$R = 3.64$ cm

$k = 0.507$ cm

$T = 490$ dynes/cm

$\rho = 13.6$ gm/cm³

$g = 980$ cm/sec²

TE₁₁₁ mode used

$L =$ length of cavity from mercury surface to the top
 $= 1.60$ cm

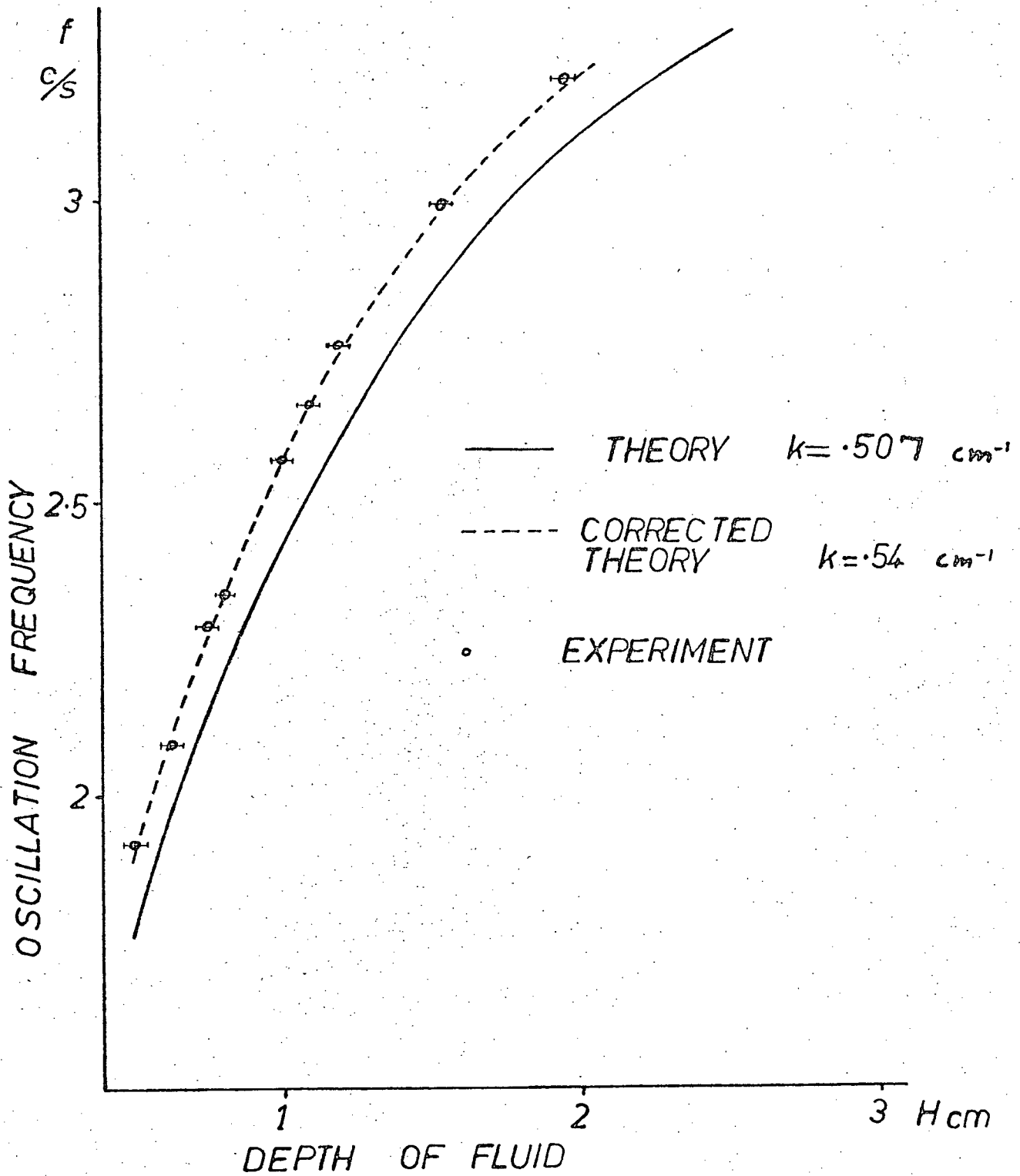


FIG 11

Plot of oscillation frequency of surface mode vs. fluid depth.

3.2. Results of the effects of application of a strong electric field on the mercury surface

One of the most sensitive tests to determine the physical properties of a liquid surface, short of examining it with an electron microscope, is to measure the damping coefficient of surface waves. This viscous damping coefficient is a most sensitive indicator of the degree of cleanliness of a liquid surface; and most physical properties of the surface depend, almost entirely, on how clean the surface is (see ref. 9). Experience in dealing with mercury surfaces has shown us that the minutest amounts of impurities tend to have a most drastic effect on the viscous damping coefficient. Even a monolayer of ordinary machine oil, obtained by spraying the oil very finely close to the surface, so that contamination occurs from the oil vapour, increases the viscous damping coefficient by a factor of 2, or even more.

Surface waves were excited by varying the frequency of the air pulses. When this frequency matched one of the surface mode frequencies (or sometimes one of the sub-harmonics) the surface oscillated with that particular frequency. The air supply was then shut off and the surface allowed to oscillate freely, the oscillation gradually damping away. A time record of this damped oscillation was obtained on the moving film. A log-linear plot of the amplitude of this damped oscillation vs. time (both obtained from the

film) resulted in a very good straight line. A typical plot is shown in fig. 12. This implies an exponential amplitude decay, exactly as predicted by the linearised theory. The slope of the straight line is the damping coefficient. The period of oscillation could be obtained very accurately by using the time markers to measure the time for a number of oscillations, usually twenty.

In our experiments, newly distilled mercury was used at the beginning. The cavity was cleaned as well as possible from dust traces. Then the clean mercury was introduced and the damping coefficient measurements performed. It was found that, even with the above steps to avoid contamination, the damping coefficient values were higher than the values theoretically predicted for clean mercury. This rather annoying effect has been observed by other workers as well (see ref. 2). It also results in very erratic and highly inconsistent values for the damping coefficient. After applying an electrostatic field of 18.5 kV/cm for a few minutes and then removing it, the values obtained for the viscous damping coefficient tended to the clean surface values. They also became much more consistent. The longer the time of application of the field the more consistent the results were. Table 3 shows the results for comparison.

After we established the cleaning of the surface by the electric field the mercury was allowed to stand in the cavity for a few days. The damping coefficient gradually

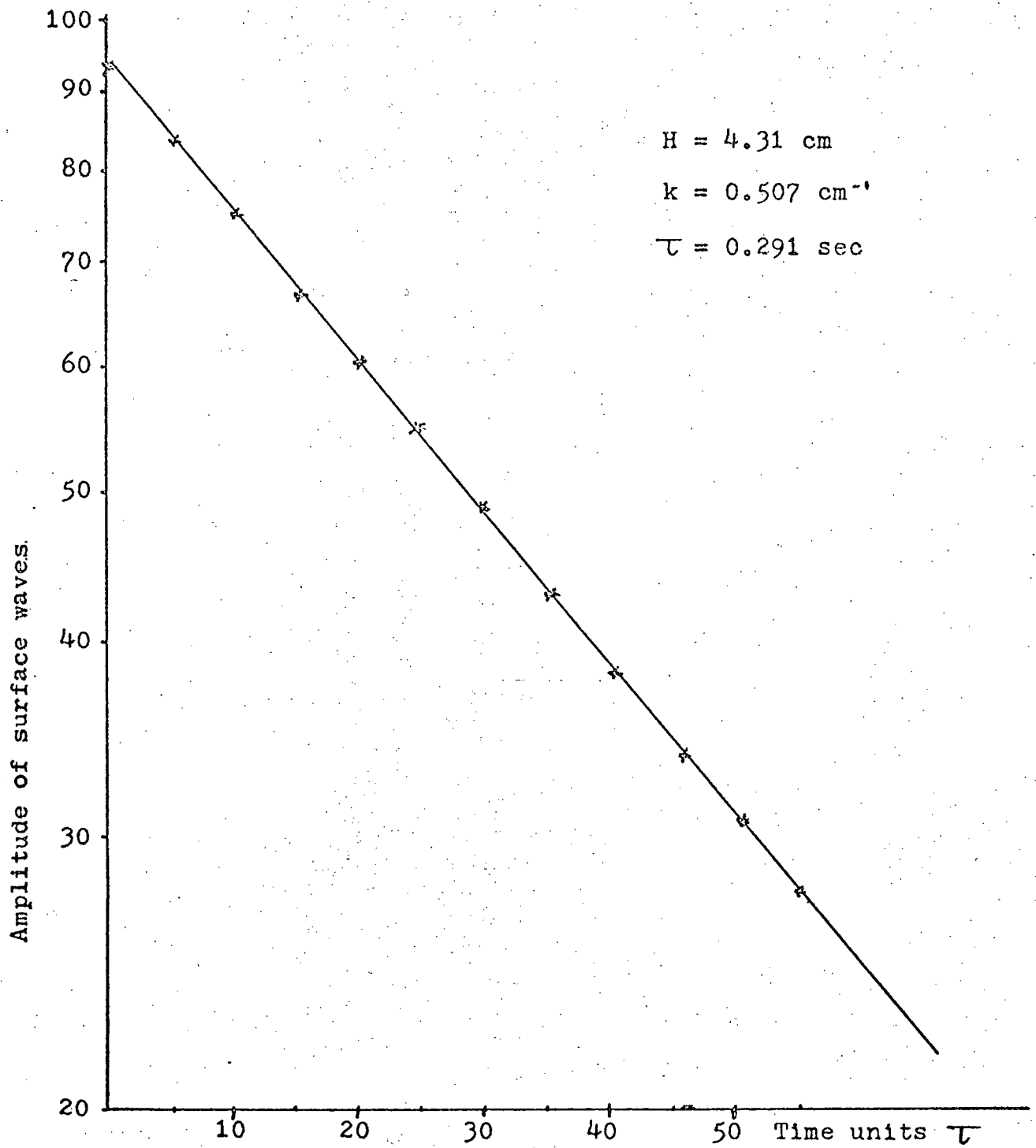


FIG 12

Exponential damping of a surface wave in time.

increased towards the "dirty surface" values, presumably because the impurities were slowly resettling on the surface. It was very encouraging indeed to find that application of the field again gave us cleaning effect.

A further test was conducted as follows. The top of the cavity was removed and a piece of cardboard which just fitted into the cylindrical cavity was inserted in the cavity just below the top. A very fine spray (an atomizer) was used to spray the rim of the cavity with ordinary machine oil. The cardboard prevented any oil droplets from settling directly on the mercury surface (see fig. 13). Thus, after removal of the cardboard, and replacement of the lid of the cavity, the surface was contaminated by minute amounts of oil vapour coming to settle onto it. The viscous damping coefficient values became even more irregular than before, and displayed a sharp increase, as can be seen from table 3. Then the field was applied as before and cleaning was again achieved after a while.

The same EM and surface mode used in the frequency measurements of 3.1 were employed in this test. The geometry of the cavity was identical and all the measurements were taken with a depth of mercury $H = 4.31$ cm.

It is seen that perfectly clean values are not attained. However, much more consistent and relatively clean surface results are obtained. By looking at the results we can state, with a certain amount of confidence, that the

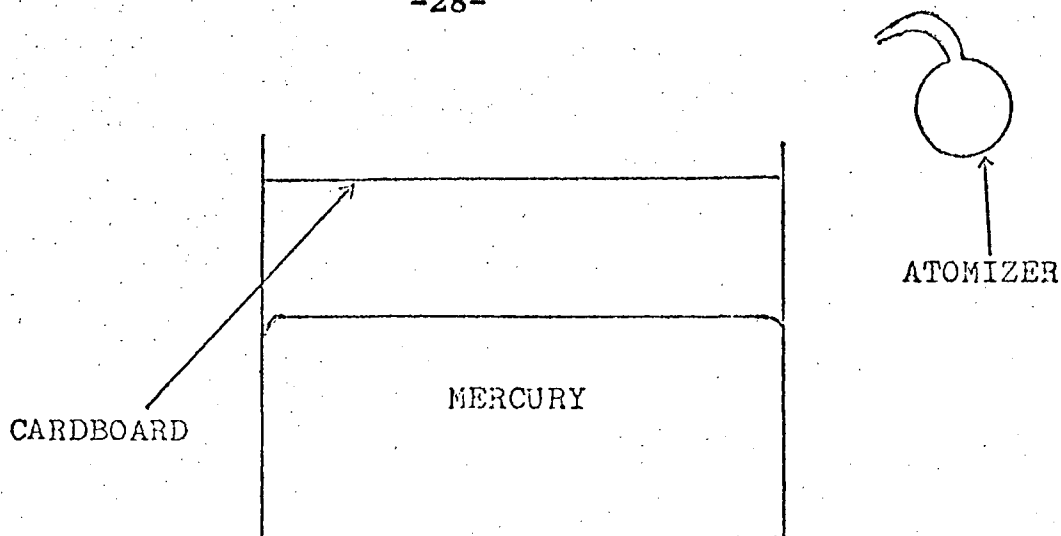


FIG 13

Method of contaminating the mercury surface with machine oil vapour.

TABLE 3

σ sec ⁻¹ Before field applied	Corresponding σ After field applied	
0.070	0.048	NO OIL
0.067	0.046	
0.079	0.045	WITH OIL
0.074	0.044	
0.112	0.044	

$$H = 4.31 \text{ cm}$$

Perfectly clean value predicted by Case and Parkinson

$$\sigma = 0.029 \text{ sec}^{-1}$$

Value predicted by the modified theory of Curzon and Pike

taking a thin, insoluble surface film into account and using corrected value of k ($= 0.54 \text{ cm}^{-1}$), $\sigma = 0.052 \text{ sec}^{-1}$.

cleaning is a little more effective when oil is spread on the surface in the manner described above. The oil most probably carries dust particles with it. Note that another use of the Mylar sheets is to prevent traces of oil from the air supply from entering the cavity and contaminating the mercury. A white gauze, used in an air filter turned dark brown after the air was run through for about an hour.

A good theoretical approach to calculating the viscous damping coefficient was given by Case and Parkinson (ref. 10). It was modified by Curzon and Pike (ref. 2) to take into account a thin insoluble film which invariably forms on all exposed liquid surfaces. This resulted in an increase in the value of the damping coefficient, giving good agreement with experiment. However, in view of the increased accuracy of the tests carried out in this project and the almost incredible discordance in observations, we must conclude that a lot more needs to be done before a clear understanding of the physical properties of a mercury surface is reached.

3.4 The rectangular cavity

Our goal in this project was to demonstrate the Fourier analyzing property of the rectangular cavity resonator.

According to theoretical work carried out by Curzon and Pike (refs. 2 and 3) there should be a selective detection of surface modes in a rectangular cavity. By using Slater's theorem (ref. 6), they showed that the shift in resonant frequency $\Delta\omega$ of an EM mode due to small perturbations of one of the surfaces of the resonator is

$$\frac{2\Delta\omega}{\omega} = \frac{\int_0^{\xi} \int B^2 dA dz}{\int_0^C \int B^2 dA dz} - \frac{\int_0^{\xi} \int E^2 dA dz}{\int_0^C \int E^2 dA dz}$$

where ω is the resonant frequency with the surface in equilibrium, ξ is the perturbation, E and B the electric and magnetic fields associated with the EM mode, dA an element of cross-sectional area (parallel to the perturbed base of the resonator in our case) and dz an element of length along the axis of the resonator. C denotes the length of the cavity. If the cavity has cross-section axb, then Lamb (ref. 8) gives the following expression for ξ

$$\xi = \sum_{s,u} \xi_{s,u} \cos\left(\frac{s\pi x}{a}\right) \cos\left(\frac{u\pi y}{b}\right)$$

where an analogous notation to the one for the cylindrical* cavity has been used. The geometry of the cavity is shown in fig. 14. Considering TE modes in the cavity (most useful ones and the ones likely to be employed), numbered TE_{mnp}

* See p. 20

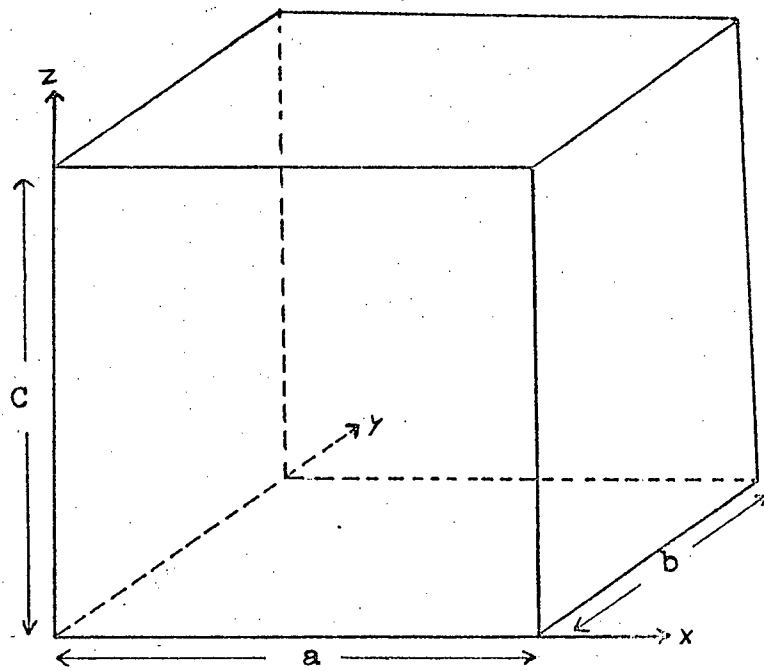


FIG 14

Geometry of the rectangular cavity resonator.

in the usual electromagnetic notation, the following expressions for $\Delta\omega$ were obtained by Curzon and Pike

$$\frac{\Delta\omega}{\omega} = \frac{1}{4} \left(\frac{P\pi c}{\omega C} \right)^2 \left[\frac{\xi_{2m,2n}}{C} + 2 \left[\frac{(mb)^2 - (na)^2}{(mb)^2 + (na)^2} \right] \left(\frac{\xi_{0,2n}}{C} - \frac{\xi_{2n,0}}{C} \right) \right]$$

where c is the velocity of light.

It is readily seen that the general EM mode TE_{mnp} depicted above will respond only to the three surface modes

$$\xi_{2m,2n}, \xi_{0,2n} \text{ and } \xi_{2m,0}.$$

This provides us with a powerful tool for doing automatic Fourier analysis of surface modes.

A cavity of square cross-section was used for this experiment. Since the cavity cannot be made exactly square, the degeneracy of the EM modes is removed sufficiently for two of them to appear separately within the bandwidth of the klystron. Hence both modes could be observed simultaneously on the oscilloscope screen. Fig. 15 shows a photograph of the klystron output on the oscilloscope screen with two EM modes observed on the screen simultaneously. If one of

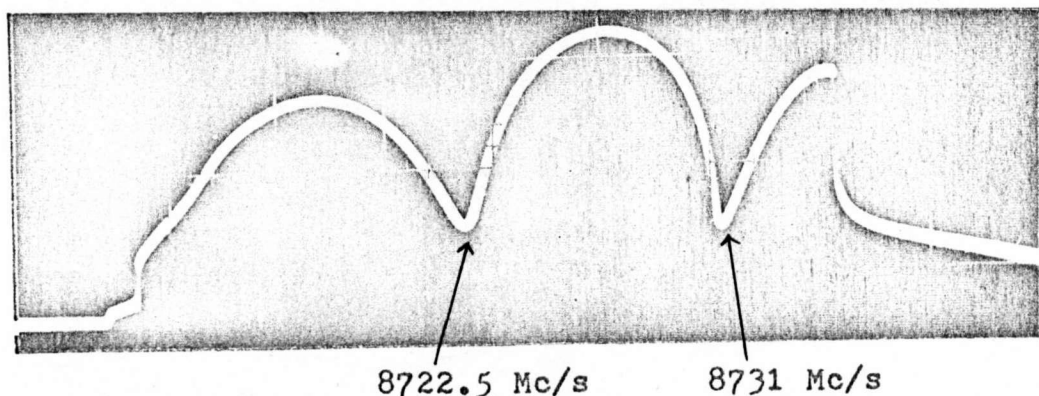


FIG 15

Display of two EM modes on the screen simultaneously.

them could be shown to respond to a surface mode while the other one did not, then the Fourier analyzing technique would have been verified.

Exactly the same experimental arrangement as for the cylindrical cavity was used. The only novelty was that in the case of the square cavity the microwaves were fed directly through the centre of the top plate, while the air was pulsed through a hole on the diagonal. The geometry is shown in fig. 16. This modification was found to increase the Q-factor of the EM modes, resulting in a sharper separation between them. Pulsing the air through an off the centre hole was no hindrance at all to the excitation of surface modes.

Various surface modes could be excited and detected as the frequency of the air pulses was gradually increased. It was observed, much to our delight, that without any difficulty we could excite resonant oscillations of the surface, to which only one of the EM modes responded. An example of one of our original films is shown in fig. 17. The EM mode dips on the screen being pretty sharp, the slit in front of the screen was so arranged as to give one trace per dip. The sinusoidal curve on the right hand side is obviously a resonant surface mode. A slight motion of the left hand dip can also be detected. It is easily recognised as the effect of "stretching" and "compressing" the klystron output curve on the oscilloscope face by the motion of the right hand dip. It is not an independent oscillation. If we

look carefully enough we can see that the left hand dip only shifts slightly to the right when the right hand dip is closest to it. The right hand oscillation effectively pulls the left hand one (notice that the left hand moves in the opposite direction to the right hand one). Fig. 18 shows a similar experiment in which both EM modes are affected by a surface mode of different geometry. In this case two clear independent oscillations can readily be seen on the film. Both films are positive enlargements of the sinusoidal curve obtained on the corresponding negative in the method described in detail in chapter 2.

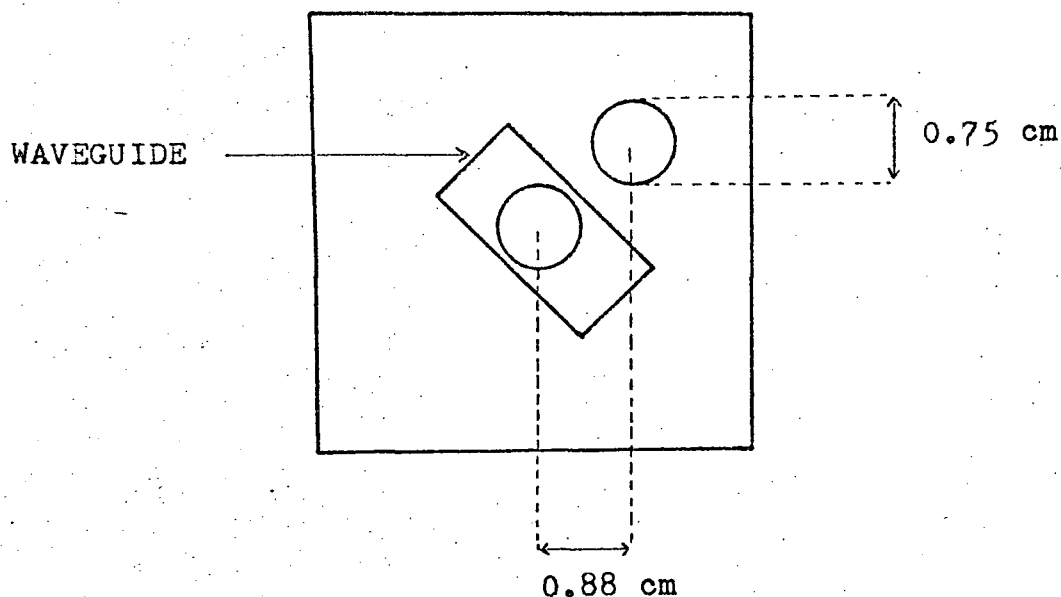


FIG 16

Geometry of the top of the rectangular cavity.

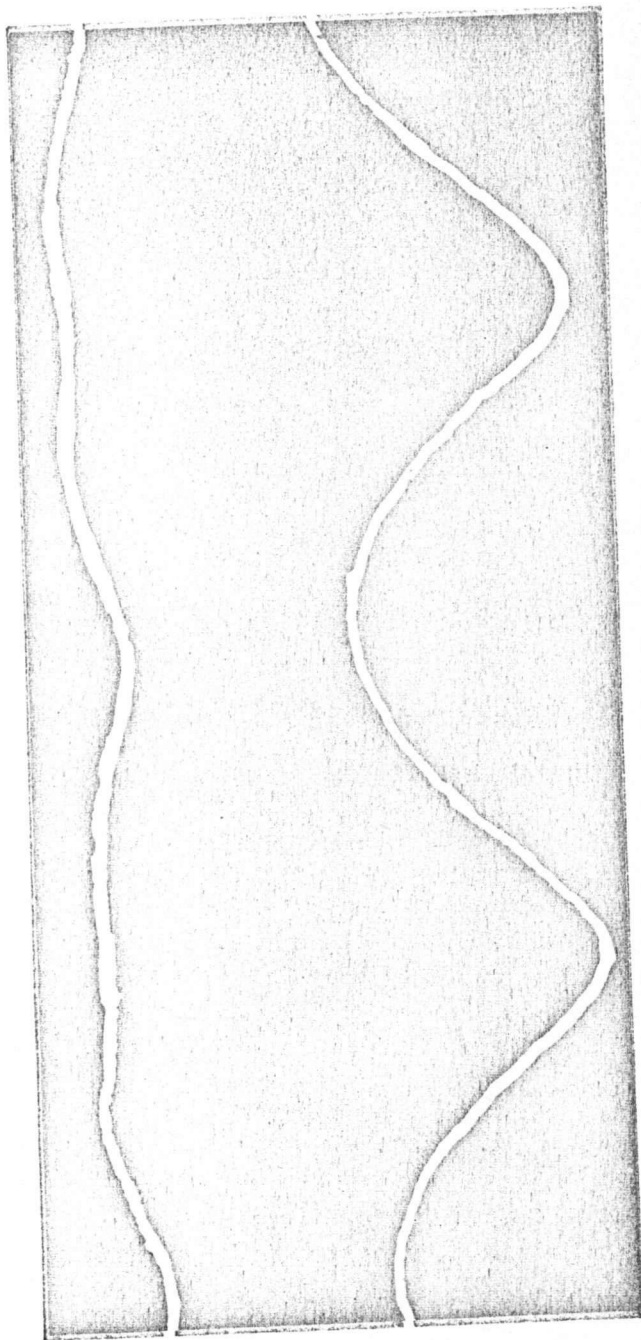


FIG 17

Response of only one EM mode to a certain surface mode.

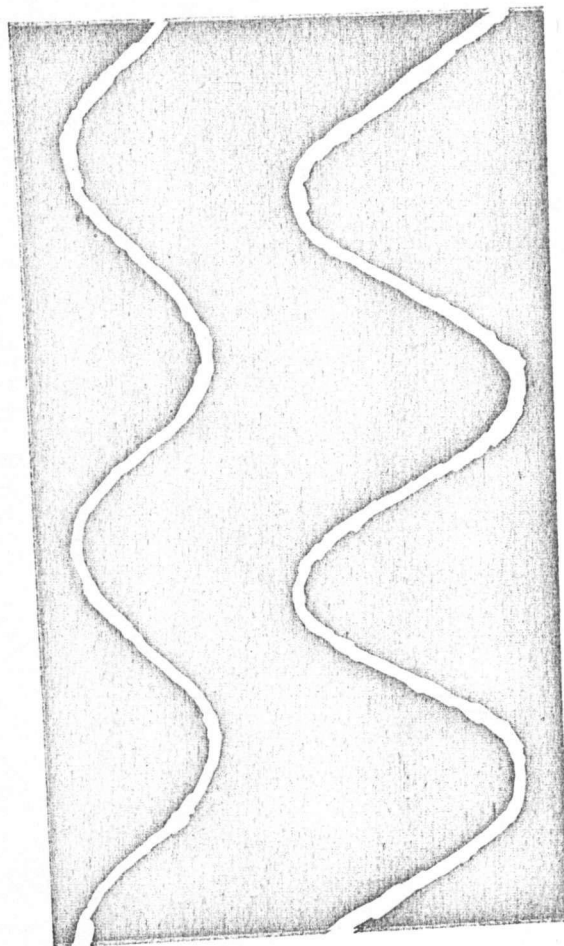


FIG 18

Response of both EM modes to a surface mode.

CHAPTER 4

CONCLUSIONS - FUTURE WORK

4.1 Improvement of measuring technique

The method of studying surface waves of small amplitude by a microwave resonator technique was improved by making the time measurement more accurate and much more convenient. It was used to check the oscillation frequency of a surface mode of different geometry from the one used before. The Curzon-Pike meniscus correction was verified. The correction obtained was more reliable than previous ones because of the improvement of the time measuring technique which gave us very accurate values for the oscillation frequency f ($= 0.1\%$).

4.2 Application of a strong electric field on the surface

The main objective of this work was to find a way of applying a strong electrostatic field onto the mercury surface without interfering with the method of monitoring surface perturbations. This was done by inserting Mylar sheets as insulators between the lid of the cavity and the base. Then the base of the cavity and the top were raised to constant potentials with a large potential difference between them. To study the electrostatic-hydrodynamic instability (ref. 7, p. 35) an increase of the field is necessary. Our calculations show that about 70 kV/cm must be obtained to get any observable effects. This will

be done by using a cavity of larger diameter than the ones so far used. This will enable us to minimize the distance between the mercury surface and the cavity lid for a given EM mode, thereby increasing the electrostatic field for a given applied potential difference. To avoid the possibility of dielectric breakdown in the cavity sulphur hexafluoride gas will be pumped into the resonator after the air is expelled.

4.3 Effect of electrostatic field on the surface

In preliminary experiments described in this thesis the effect of a strong electric field on the properties of the mercury surface was demonstrated. A method for removing traces of contamination from the surface was found. This can prove very useful to physicists and physical chemists. Their observations have so far been plagued by irreproducibility due to the great sensitivity of liquid surfaces to contamination.

4.4 Square resonator

The feasibility of using a rectangular resonator as an automatic Fourier analyzer was demonstrated by using a square cavity. This is a very important property of the resonator technique for studying surface waves, since dispersion relations can be measured directly, thereby eliminating Fourier analysis.

4.5 Possibility of applying the method in other fields

A final aspect of the method as a whole, on which we would like to comment, is the following. This method of observation of disturbances on a fluid surface can, in principle, be employed as a seismometric device. An old method of detecting earthquakes was by observing the disturbances on the surface of water in a well resulting from the earthquake. In a similar manner, the more sophisticated microwave resonator technique can be used as an earthquake detector. It combines the two basic features of a seismograph. Firstly, it is extremely sensitive. This was clearly demonstrated by our being able to excite waves on the surface even with the Mylar sheets in position in the path of the air pulses. Secondly, conventional seismographs have amplification factors between 10^2 and 10^5 , depending on their purpose (see ref. 11). Our system amplifies waves of 0.001 in. to motions of about 2 to 3 inches on the oscilloscope screen, i.e. an amplification of 2 to 3 thousand, right inside the range. Finally, since the Fourier analyzing property of rectangular resonators has been demonstrated, they can be employed to Fourier analyze an earthquake signal automatically. At present, the Fourier analysis of seismograms takes up a lot of energy of personnel manning seismographs.

REFERENCES

1. Curzon, F. L. and Howard, R. (1961), Can. Journal of Physics 39, 1901.
2. Pike, R. L. (1967), Ph.D. Thesis, University of British Columbia, Department of Physics.
3. Curzon, F. L. and Pike, R. L. (1968), Can. Journal of Physics 46, 2001.
4. Curzon, F. L. and Pike, R. L. (1968), Can. Journal of Physics 46, 2009.
5. Curzon, F. L. and Pike, R. L. (1969), Can. Journal of Physics 47, 1051.
6. Slater, J. C. (1963), Microwave Electronics, Bell Laboratories Series.
7. Landau, L. D. and Lifshitz, E. M. (1960), Electrodynamics of Continuous Media, Addison-Wesley.
8. Lamb, H. (1945), Hydrodynamics, Dover Publications Inc., New York.
9. Burdon, R. S. (1949), Surface Tension and the Spreading of Liquids, Cambridge University Press.
10. Case, K. M. and Parkinson, W. C. (1956), J. of Fluid Mechanics 2, 172.
11. Richter, C. F. (1958), Elementary Seismology, W. H. Freeman, San Francisco.
12. Ries, H. E. Jr., and Kimball, W. A. (1957), Proceedings of the Second International Congress of Surface Activity, Vol. I, Butterworths Scientific Publications, London.

APPENDIX

THEORY OF THE CLEANING OF THE MERCURY SURFACE BY THE APPLICATION OF A STRONG ELECTROSTATIC FIELD

Our purpose in this appendix is to propose a theoretical explanation of the cleaning effect that the strong electrostatic field has on the mercury surface. Before proceeding, we would like to warn the reader that, as any textbook of Physical Chemistry will convey, the physical principles behind the behaviour of liquid surfaces are still not fully and clearly understood. Their behaviour is so intricate and complicated, and experimental techniques so difficult when it comes to studying the actual surface, that a lot of work has still to be carried out before any general picture of the numerous aspects of the surfaces can be given. What we shall suggest below is a simple physical model of the cleaning process.

A liquid surface, when formed by pouring perfectly pure liquid in a container, soon forms a thin, insoluble film on itself. This is composed of traces of grease that are in the container or in the atmosphere above the surface, very fine dust particles, or even oxides. The effect on the physical properties of the surface is more pronounced when contaminated with oil as was described in the previous chapter. So we

shall treat this more general case in our theoretical argument.

Our method of contamination of the mercury surface with oil will result in the formation of a collapsed monolayer of oil on the surface. By a collapsed monolayer we mean a layer of oil of molecular thickness (of the order of 10 Å), on which clusters of oil molecules forming extremely fine droplets (not visible to the naked eye) are found at random positions on the surface (see fig. 19a). A mechanism for the formation of the collapsed monolayer can be found in ref. 12, p.75 to p.84. This film is so thin that the surface charge on the conductor (mercury) resulting from the application of the field can be considered to reside on it. At fields of about 20 kV/cm like the ones employed in the tests there will be large electrostatic stresses on the thin oil film. If we consider an oil droplet of, for convenience sake, hemispherical shape (fig. 19b) of radius r , we can readily visualize the simple cleaning mechanism. Due to the surface stress trying to pull on the oil film a deformation will occur when the field is applied and the configuration of fig. 19c will be assumed. The weight of the droplet, cohesive forces exerted by neighbouring oil molecules and adhesive forces exerted by the mercury will tend to pull it back into position. The equation for the balance of forces can be written as

$$\frac{\epsilon_0 E^2}{2} \cdot 2\pi r^2 = 2\pi r F \sin\theta + F_{ad} \pi r^2 + \rho \cdot \frac{2}{3} \pi r^3 g \quad (A.1)$$

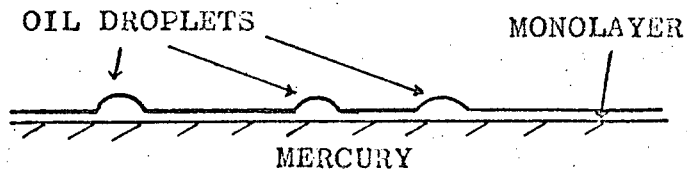


FIG 19

A collapsed monolayer of oil on the mercury.

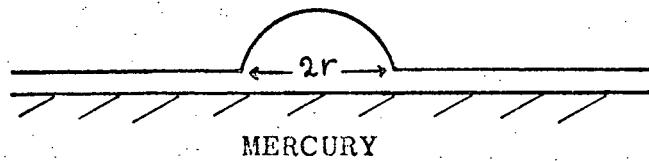


FIG 20a

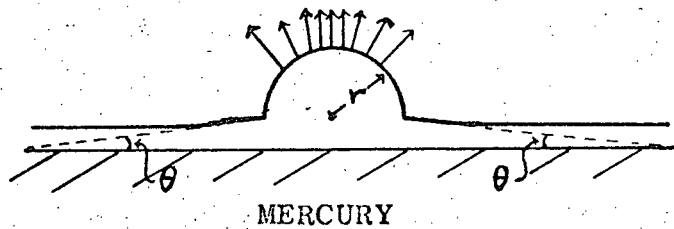


FIG 20b

Mechanism of the removal of contaminants from the mercury surface by a strong electric field.



FIG 21

Mechanical analogue of the breaking up of the thin oil film.

where F = cohesion force per unit length,

F_{ad} = adhesion force per unit area

ρ = density of oil

E = electrostatic field

and g = acceleration of gravity.

Therefore

$$2F = \left(\epsilon_0 E^2 - F_{ad} - \rho \frac{2}{3} g r \right) \frac{r}{\sin \theta} \quad (\text{A.2})$$

But since θ is a very small angle F can become a very large force. So large in fact that cohesion effects will not be able to supply it and the oil film will break. Under the upward acceleration of the field the oil will be accelerated upwards and will stick to the Mylar sheets at the top. Notice that only micrograms of oil are involved so it is quite easy for the field to accelerate the oil upwards. This is easily seen by the fact that the stress on the oil surface at fields of 20 kV/cm is

$$\epsilon_0 E^2 = 8.85 \times 10^{-12} \times 4 \times 10^{12} \text{ Nt.} = 354 \text{ dynes} \quad (\text{A.3})$$

A mechanical analogue of the breaking up of the oil film is the case of a small weight attached to the centre of a nearly horizontal string as shown in fig. 20. Even if the weight is quite small the tension in the string will be enormous for very small θ .